9th US National and 10th Canadian Conference on Earthquake Engineering: *Reaching Beyond Borders*
toronto july 25-29, 2010
9ième Conférence Nationale Américaine et 10ième Conférence Canadienne de Génie Parasismique: *Au delà des Frontières*

Conference Co-Sponsors
Earthquake Engineering Research Institute
The Canadian Association for Earthquake Engineering
L'Association Canadienne du Génie Parasismique

STIFFNESS ANALYSIS OF FIBER-REINFORCED RUBBER ISOLATORS UNDER COMPRESSIVE LOADS: A FINITE ELEMENT APPROACH

H. Toopchi-Nezhad [1], M.J. Tait[2], and R.G. Drysdale[3]

ABSTRACT

Fiber reinforced elastomeric isolators (FREIs) can be effectively used for seismic mitigation of structures. In contrast to conventional steel reinforced elastomeric isolators (SREIs), FREIs are significantly lighter in weight, and can be fabricated in a cost-effective manner. Unlike SREIs, the reinforcement layers in FREIs are flexible in extension and have no bending rigidity. As a result, the response characteristics of FREIs are different, and in general more complex than those corresponding to SREIs. Due to the fiber flexibility, the theoretical approach employed in the stiffness analysis of SREIs cannot be directly extended to FREIs. Analytical closed-form techniques for stiffness solution of FREIs under vertical pressure have been presented in the literature. There is a need to compare these solutions with more rigorous numerical techniques. In this paper, a finite element approach has been employed to investigate the static response of a strip FREI under a compressive vertical load. A hyperelastic model has been used for the rubber material in the finite element code. Results of the finite element analysis, including compression stiffness and stress distributions in the elastomeric layers, have been compared with those predicted by the closed form analytical solution.

Introduction

Fiber reinforced elastomeric isolators (FREIs) consist of alternating bonded layers of elastomer and fiber reinforcement. In contrast to steel reinforced elastomeric isolators (SREIs), FREIs are significantly lighter in weight and potentially more cost effective if fabricated through a

[1]Post Doctoral Fellow, Dept. of Civil Engineering, McMaster University, Hamilton, ON, L8S 4L7
[2]Associate Professor, Dept of Civil Engineering, McMaster University
[3]Professor Emeritus, Dept. of Civil Engineering, McMaster University

mass production manufacturing technique.

Previous research has confirmed the effectiveness of FREIs in seismic isolation of typical low-rise structures (Toopchi-Nezhad et al. 2009). The role of fiber reinforcement in a FREI is primarily to provide vertical stiffness by limiting the lateral bulging of the elastomeric layers when the isolator is subjected to vertical compressive loads. It should be noted that the reinforcing steel plates play the same role in conventional SREIs. However, unlike the steel reinforcement in a SREI, which is rigid in elongation and has significant bending rigidity, fiber reinforcement in a FREI is flexible in extension and has negligible bending rigidity. Therefore, the response characteristics of a FREI in both the vertical and horizontal directions are significantly different than a corresponding SREI. Consequently, current analytical solutions derived for SREIs cannot be directly extended to FREIs.

The "pressure solution" is a commonly used analytical approach in predicting the vertical stiffness of conventional SREIs (Kelly 1997). A modified version of this analytical approach which accounts for the in-plane tension flexibility of the fiber reinforcement has been developed for the vertical stiffness evaluation of FREIs (Kelly 1999). This paper presents a detailed comparison between the results of the "pressure solution" and finite element analysis by investigating the vertical stiffnesses of infinitely long strip FREIs under constant compressive load. The main research objective is to verify the accuracy of the "pressure solution" in vertical stiffness analysis of strip FREIs reinforced with fiber reinforcement layers of different in-plane tensile rigidity. The physical and material properties of the elastomeric layers are identical for all FREIs considered in this study.

Pressure Solution

The "pressure solution" (Kelly 1997) is commonly used for stiffness analysis of conventional SREIs under vertical compressive loads. This method assumes that the elastomeric material in the isolator is linear elastic. Additionally, as an elastomeric layer in a SREI is laterally confined by the rigid steel reinforcing plates, the deviatoric component of normal stresses in the elastomer is neglected. Therefore, noting the coordinate system shown in Fig. 1, the stress state in an infinitely long elastomeric layer is characterized by $\sigma_{xx} \approx \sigma_{zz} = p$ (where, p is an internal pressure), and $\tau_{xz} \neq 0$. The pressure p is obtained by solving a partial differential equation resulting from the equilibrium of stresses and the constraint of incompressibility in the elastomer.

The "pressure solution" approach has been also employed in vertical stiffness analysis of FREIs (Kelly 1999). However, the solution has been modified to account for the stretching of fiber reinforcement layers, which cannot be neglected in the analysis. Figure 1 shows the sketch of a single elastomeric layer of width $2a$ and thickness t, which is bonded between two reinforcement layers forming an infinitely long rectangular pad. In a typical elastomeric isolator of plan area A consisting of n pads with a total thickness of elastomeric layers of $t_r = nt$, the vertical stiffness, K_v, is defined as (Kelly 1997)

$$K_v = \frac{E_c A}{t_r} \tag{1}$$

In Eq. 1, E_c, the effective compression modulus of the strip FREI, using "pressure solution" approach is given by (Kelly 1999, Tsai and Kelly 2002):

$$E_c = \frac{12GS^2}{(\alpha a)^2}\left(1 - \frac{\tanh \alpha a}{\alpha a}\right) \tag{2}$$

with

$$\alpha a = \frac{a}{t}\sqrt{12\frac{Gt}{k_f}} \tag{3}$$

where, a is half the isolator's width, t is the thickness of the elastomeric layer, $S = a/t$ reflects a shape factor index, G is shear modulus of the elastomer, and k_f is the in-plane tension stiffness of the fiber reinforcement, which is defined based on E_f (Young's modulus), t_f (thickness), and υ_f (Poisson's ratio) as follows

$$k_f = E_f t_f / (1 - \upsilon_f{}^2) \tag{4}$$

Equation 2 is expected to be reasonably accurate for FREIs having shape factors ranging between 5 and 15 (Kelly 2002). It should be noted that for conventional strip SREIs, the "pressure solution" leads to an effective compression modulus of $E_c = 4GS^2$ (Kelly 1997).

The distribution of internal pressure, p, along the width of the FREI is given by Kelly (1999) as:

$$p(x) = -\frac{\delta}{t}\frac{E_f t_f}{t}\left(1 - \frac{\cosh \alpha x}{\cosh \alpha a}\right) \tag{5}$$

where δ represents the vertical deflection of a single elastomeric layer in the isolator.

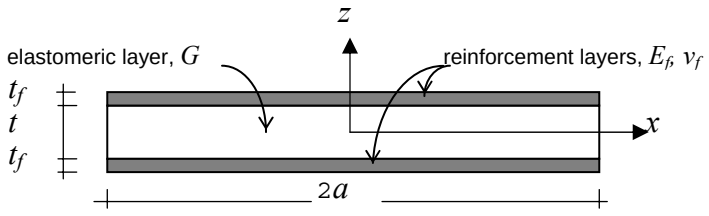

Figure 1. Sketch of an infinitely long rectangular pad

The Strip FREIs Considered in this Study

In order to verify the accuracy of the "pressure solution" and to study the role of fiber reinforcement in the vertical stiffness of FREIs, six isolators with different k_f / Gt values were investigated. The ratio of k_f / Gt indicates the relative in-plane tension stiffness of the fiber reinforcement to the shear stiffness of the elastomeric layer. The values for k_f / Gt selected in this study were $10, 10^2, 10^3, 10^4$, and 10^5. Each isolator contained eleven $10mm$ thick rubber layers interleaved with ten fiber reinforcement layers. All isolators were subjected to a mean vertical pressure of $p_m = 3MPa$. The material properties of fiber reinforcement were characterized with $E_f = 137GPa$ and $\upsilon_f = 0.2$. Shear modulus of the elastomer was assumed to be $G = 0.4MPa$. The width and height of the individual elastomeric layers in all of the isolators were $200mm$ and $10mm$, respectively. This leads to an identical shape factor of $S = 10$ for all of the isolators which falls within the accepted range of shape factors for application of the pressure solution (Kelly 2001). Therefore, for the isolators investigated, the pressure solution results can be reasonably compared with the finite element solutions.

Finite Element Approach

The finite element analysis was carried out using Abaqus software (Abaqus Theory Manual 2007). Nonlinear elasticity of the elastomeric material was simulated using a Neo-Hookean hyperelastic material model provided in Abaqus. Given the $0.4MPa$ shear modulus of the elastomer and its bulk modulus of $2000MPa$, the Neo-Hookean coefficients were calculated to be $c_{10} = 0.2$, and $D_1 = 0.001$. The elastomeric layers were discretized using 4-node bilinear, plane strain, quadrilateral, hybrid, constant pressure solid elements called CPE4H. The fiber reinforcement was modeled using 2-node linear 2D truss elements called T2D2 (Abaqus Theory Manual 2007).

Two rigid contact supports were defined at the top and bottom of the isolators. All of the degrees of freedom of the bottom support were fixed. The top support was allowed to move in the vertical direction only. A concentrated vertical load was applied at the center of the top support.

The elastomeric layers were discretized using two different finite element meshes to study the sensitivity of the results to the size of the finite elements. Mesh 1 contained $2.5 \times 1.25\ mm$ solid elements (a total of 640 elements for each elastomeric layer) whereas Mesh 2 employed finer elements of $2 \times 1\ mm$ (1000 elements per elastomeric layer). The aspect ratio of elements for both meshes was 2. A difference of less than 0.3% was found in the stress values along the length of the elastomeric layers. Therefore, Mesh 1 was selected in this study.

Analysis Results and Discussion

In the finite element analysis conducted in this study, the applied vertical load was linearly increased from zero to its target value corresponding to a mean vertical pressure of $p_m = 3MPa$. Figure 2 shows the relationship between compressive stress (mean pressure) and vertical strain. The vertical strain is evaluated by dividing the total vertical deflection, Δ, by the total thickness of elastomeric layers in the isolator, i.e., $t_r = 110mm$. As can be seen in Fig. 2, for $k_f / Gt \le 1000$, vertical stiffness of the isolator increases significantly with an increase in the in-plane stiffness of the fiber reinforcement. However, for $k_f / Gt > 1000$ the rate of increase in the isolator vertical stiffness rapidly diminishes and at $k_f / Gt = 10{,}000$, additional increase in the in-plane stiffness of the fiber reinforcement has no appreciable influence on isolator vertical stiffness.

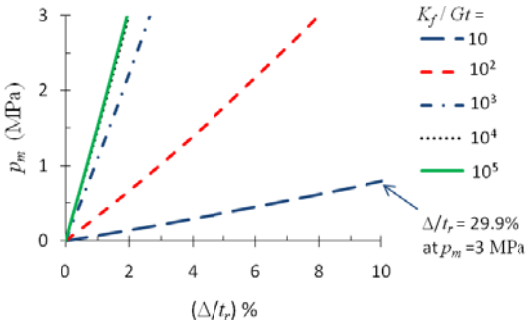

Figure 2. Relationship between mean vertical pressure, p_m, and vertical strain, Δ / t_r, for different values of k_f / Gt

A comparison between analytical (Eq. 2) and numerical (finite element) values of the isolators' effective compression moduli can be found in Fig. 3. Isolator compression moduli in this figure are normalized to the compression modulus of a corresponding isolator with infinitely rigid reinforcement layers. As can be seen in Fig. 3 the plotted curves follow a similar trend although some discrepancies exist. The maximum discrepancy between the two methods occurs at $k_f / Gt = 10$ where the pressure solution underestimates E_c by 63%. This underestimation decreases to 24% and 5% for k_f / Gt values of 100 and 1000, respectively. The difference between the pressure solution and finite element results at $k_f / Gt \ge 10{,}000$ is less than 2% which indicates excellent correlation between the two methods.

The thickness of steel plates in a SREI is typically not less than $3mm$. If the fiber reinforcement layers of the strip isolator considered in this study were replaced with steel plates of $3mm$ thickness, the relative in-plane stiffness of the steel reinforcing plates to shear stiffness of the elastomeric layers (i.e., k_f / Gt) would have been approximately 1.65×10^5. For such a

case, $E_c / 4GS^2$ would be very close to 1. Consistently, $E_c / 4GS^2$ in a FREI approaches unity as k_f / Gt values become quite large (see Fig. 3). Results of the finite element analysis indicate that at k_f / Gt of 10^4 and 10^5, the ratio of $E_c / 4GS^2$ reaches 0.94 and 0.98, respectively, which is close to unity.

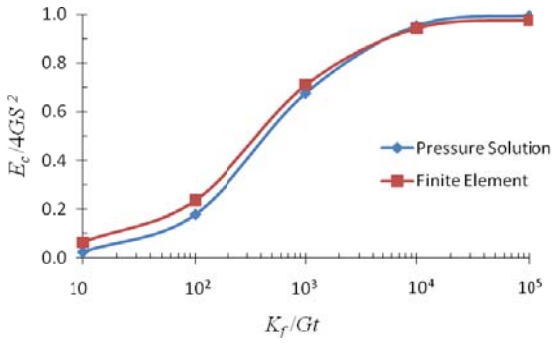

Figure 3. Variation of isolator effective compression modulus with k_f / Gt

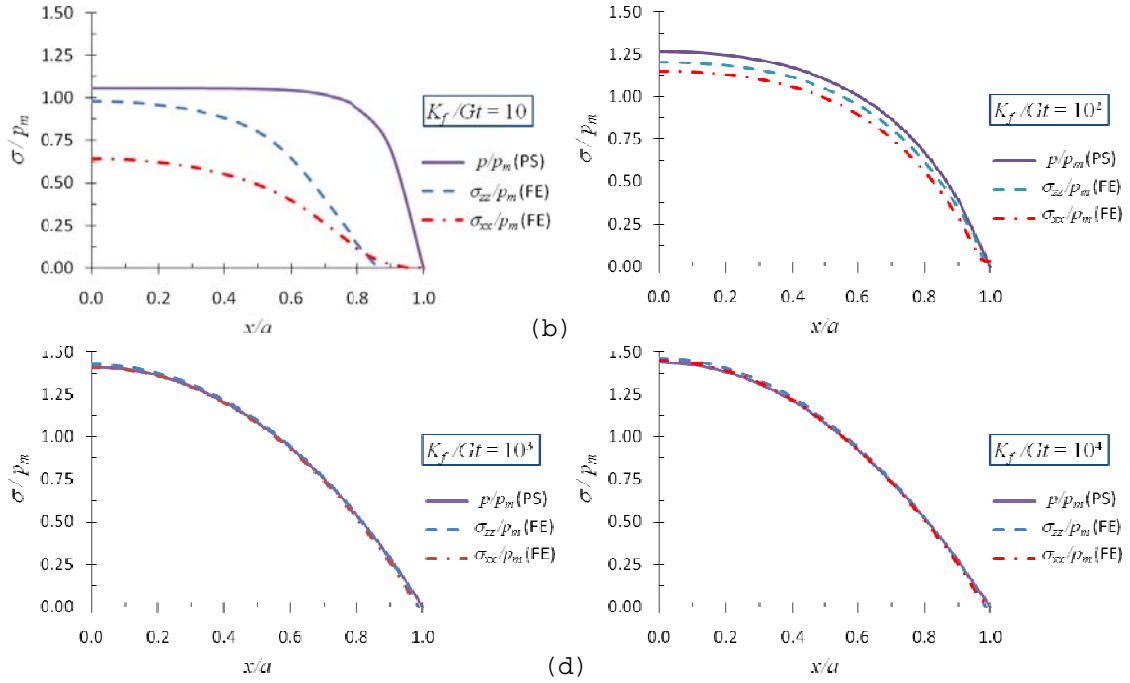

Figure 4. Results of the pressure solution (PS), and finite element (FE) analysis; distribution of the normalized stresses along the half width of an elastomeric layer located at the mid-height of the isolators with k_f / Gt values of ; (a) 10 ; (b) 10^2 ; (c) 10^3 ; (d) 10^4

Figures 4a to 4d show the distribution of normal stresses along the width of the

elastomeric layer located at the mid-height of the isolator. The normal stresses σ_x or σ_z in these figures were calculated by the finite element analysis and the internal pressure p was evaluated by the pressure solution. All stress components in Figs. 4a to 4d were normalized to the mean vertical pressure of $p_m = 3MPa$. In addition, due to symmetry, stress values are shown over the half width of the elastomer layer.

A key assumption in the pressure solution is that both horizontal and normal stresses are equal to the internal pressure p given by Eq. 5. The accuracy of the pressure solution is highly dependent on the validity of this assumption. Figure 4a indicates that due to the significant in-plane flexibility of the fiber reinforcement in an isolator with $k_f / Gt = 10$, the distribution of normal stresses σ_x and σ_z along the half width of the elastomeric layer are significantly different and the internal pressure p, calculated by the pressure solution does not match either σ_x or σ_z (See Fig. 4a). Therefore, the pressure solution in this particular case would not provide a good estimate of the isolator's vertical stiffness. Given the applied mean average pressure of $p_m = 3MPa$, the effective vertical frequency of the FREIs with k_f / Gt values of 10 and 100 were calculated to be 2.7 Hz, and 5.3 Hz, respectively. However, since these values are not sufficiently large for typical seismic isolation applications, FREIs with k_f / Gt values of 10 and 100 are deemed impractical.

According to Fig. 4b for an isolator with $k_f / Gt = 100$, although the distributions of all stress components of σ_x, σ_z and p are fairly consistent, the numerical values are not in very close agreement. Therefore, for this isolator, the pressure solution would not provide completely accurate result.

As shown in Figs. 4c and 4d for the isolators with $k_f / Gt \geq 1000$, excellent agreements between both the distributions and between the numerical values of stresses σ_x, σ_z, and p are observed. As mentioned previously in this section, in this k_f / Gt range, the isolators' effective compression moduli calculated by the pressure solution differ by less than 5%.

Figures 5a to 5d contain σ_{zz} stress contours plotted on the deformed shape of the isolators with k_f / Gt values ranging from 10 to 10^4. As shown in Figs. 5a, 5b, and Fig. 2, the FREIs with $k_f / Gt < 1000$ undergo relatively large vertical deflections and lateral expansions.

Figures 6a and 6b compares the distributions of normal stresses along the half width of the first elastomeric layer located at the bottom of the isolator (R1) with that of the elastomeric layer R6 located at the mid-height of the isolator.

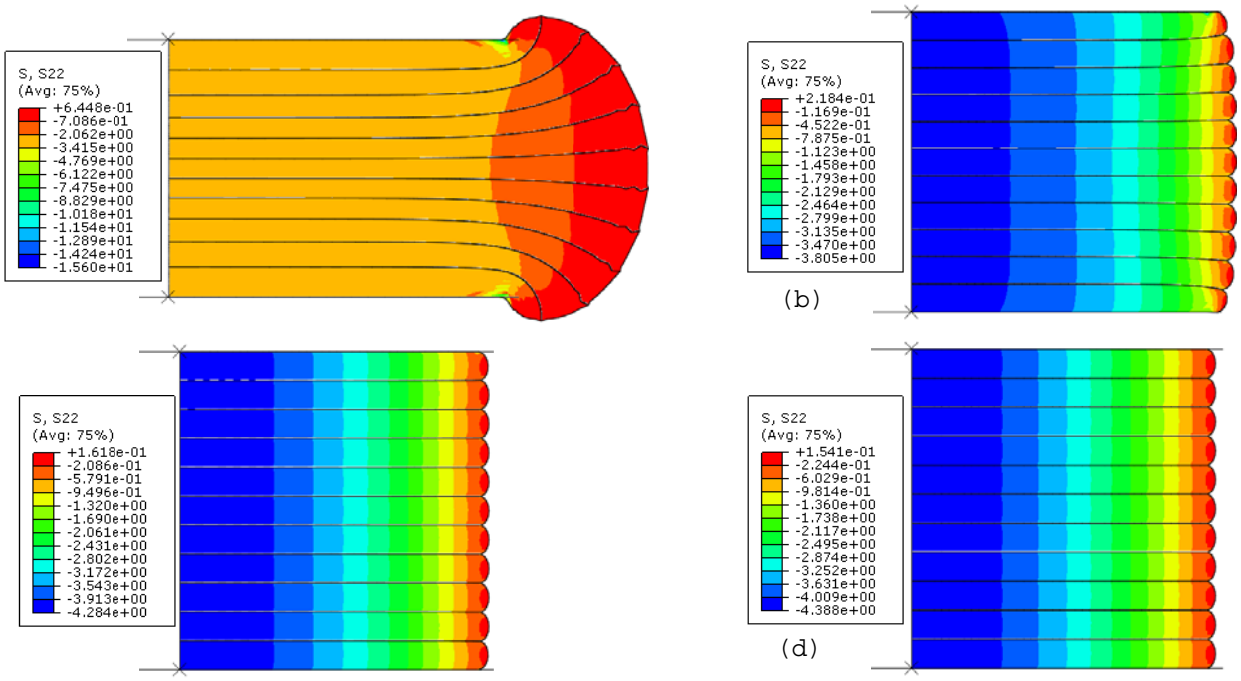

Figure 5. Stress contours for $\sigma_{zz}(MPa)$ plotted on the deformed shape of the isolators with k_f/Gt values of; (a)10; (b)10^2; (c)10^3; and (d)10^4; only half width of the isolators are shown due to symmetry

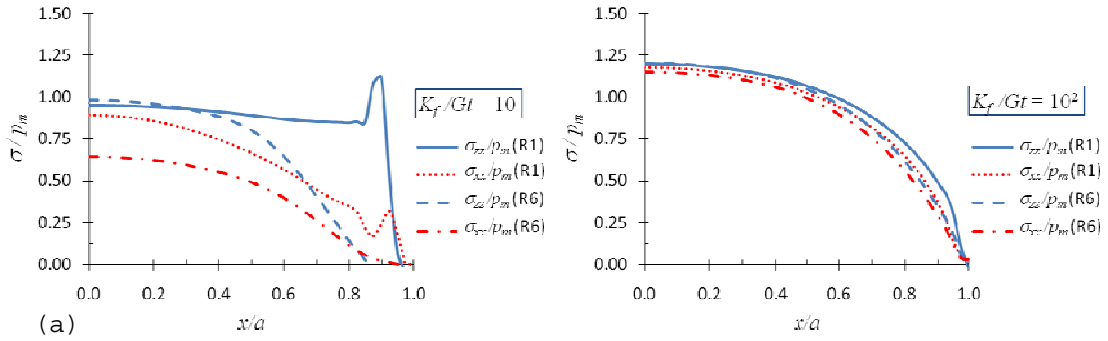

Figure 6. Distribution of vertical and horizontal stresses of σ_{zz} and σ_{xx} along the half width of elastomeric layers R1 and R6 located at the bottom and mid-height of the isolators, respectively; (a) $k_f/Gt=10$; (b) $k_f/Gt=10^2$

According to Fig. 6a for the isolator with $k_f/Gt=10$, the stress distribution in elastomeric layer R1 is significantly different than layer R6. This is expected as there was considerable difference in the deformation patterns of layers R1 and R6 in Fig. 5a. As k_f/Gt

increases, the difference in the stress distribution becomes negligible. At $k_f / Gt \geq 10^3$, the stress distributions for both horizontal stress σ_{xx} and vertical stress σ_{zz} are identical regardless of the location of the elastomeric layer in the isolator. This finding indicates agreement with the basic assumptions made with the pressure solution.

The distributions of normalized stresses σ_{zz} / p_m and σ_{xx} / p_m through the thickness of the elastomeric layer R6 located at the mid-height of the isolators are shown in Figs. 7a to 7d for various k_f / Gt values. The stress values are shown for both the mid-length (isolator's middle), and the edge (isolator's edge) of the elastomeric layer. Inspection of these figures shows that the stresses vary significantly over the thickness of the elastomer at the edge of the isolator. However, at the middle of the elastomeric layers the stress remains almost constant with negligible variation through the elastomer thickness.

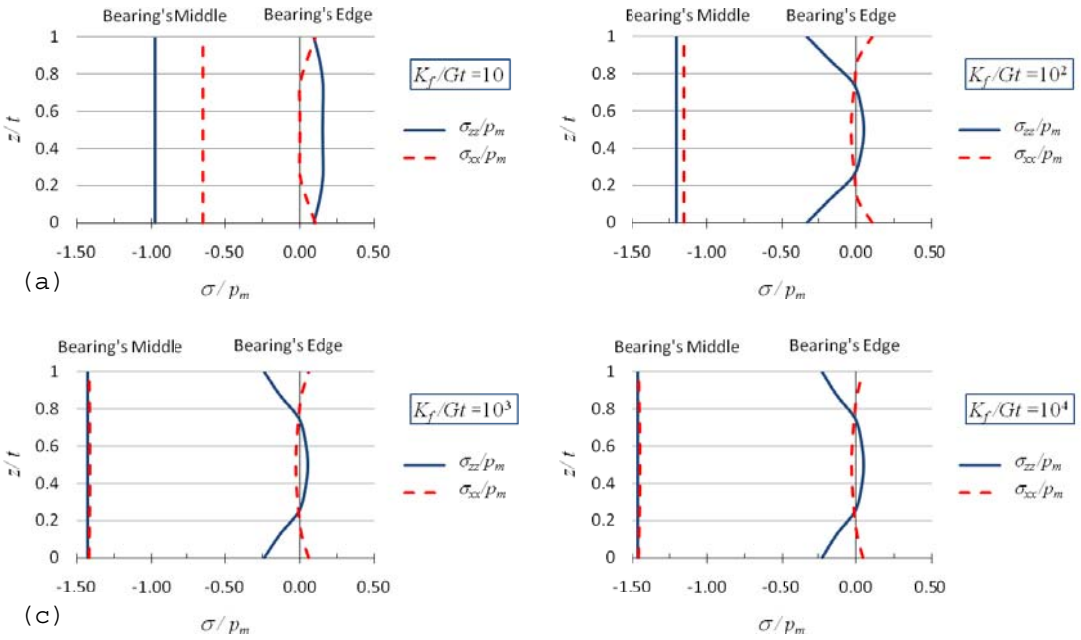

Figure 7. Variation of stresses σ_{zz} and σ_{xx} over the thickness of elastomeric layer R6 located at the mid-height of isolators with k_f / Gt values of ; (a) 10; (b) 10^2; (c) 10^3; and (d) 10^4; negative stress values indicate compression

Summary and Conclusions

The stress distributions and vertical stiffnesses of five different strip FREIs under a constant vertical compressive load were evaluated using a simplified analysis known as the "pressure solution". These were subsequently compared with finite element analysis results. A Neo-Hookean hyperelastic material model was used for the elastomeric layers of the isolators in the finite element analysis. The isolators were identical in terms of physical dimensions and

material properties. However, the in-plane tension rigidity of the fiber reinforcement in the isolators was varied. The ratio of in-plane tensile stiffness of the fiber reinforcement to the shear stiffness of the elastomeric layer, namely, k_f / Gt, was used as an index to differentiate the isolators under consideration. The shape factor, S, defined as the plan area of a single elastomeric layer to its load free perimeter area, was 10 for all isolators studied. At this S value the "pressure solution", which accounts for the stretching of fiber reinforcement layers, is thought to provide sufficiently accurate solutions.

Analysis results indicate that, for FREIs with fiber reinforcement of relatively low stiffness (i.e., $k_f / Gt < 1000$), results of the pressure solution and the finite element are significantly different. For isolators with intermediate stiff fiber reinforcement, results of the "pressure solution" were found to be reasonably accurate. Excellent correlation between the two methods was obtained for the isolators with $k_f / Gt \geq 10^4$. Although the employed pressure solution accounts for the stretching of fiber reinforcement in the FREIs, its accuracy is not independent of the in-plane flexibility of the reinforcement layers.

Acknowledgments

This research was carried out as part of the mandate of the McMaster University Centre for Effective Design of Structures funded through Ontario Research and Development Challenge Fund. The authors also would like to gratefully acknowledge the Natural Sciences and Engineering Research Council of
Canada (NSERC).

References

Abaqus Theory Manual, 2007. Abaqus Inc. and Dassault Systèmes (DS), Version 6.7, Providence, RI.

Kelly, J. M., 1997. *Earthquake-Resistant Design with Rubber*, 2nd edition, Springer-Verlag, London.

Kelly, J. M., 1999. Analysis of Fiber-Reinforced Elastomeric Isolators, *Journal of Seismology and Earthquake Engineering (JSEE),* 2(1), 19-34.

Kelly, J. M., 2002. Seismic Isolation Systems for Developing Countries, *Earthquake Spectra,* 18(3), 385–406.

Toopchi-Nezhad, H., Tait, M. J., and Drysdale, R. G., 2009. Shake Table Study on an Ordinary Low-Rise Building Seismically Isolated with SU-FREIs (Stable Unbonded Fiber-Reinforced Elastomeric Isolators), *Earthq. Engng. & Struct. Dyn.*, 38(11), 1335–1357.

Tsai, H. C., and Kelly, J. M., 2002. Stiffness Analysis of Fiber-Reinforced Rectangular Seismic Isolators, *Journal of Engineering Mechanics*, 128(4), 462- 470.